Am J Cancer Res 2023;13(10):4783-4793
www.ajcr.us /ISSN:2156-6976/ajcr0151735

Original Article

Radiation-induced skin and heart toxicity in patients with breast cancer treated with adjuvant proton radiotherapy: a comparison with photon radiotherapy

Ching-Chuan Hsieh[1*], Chi-Chang Yu[2*], Chia-Hui Chu[2], Wen-Cheng Chen[3], Miao-Fen Chen[3]

[1]Department of General Surgery, Chang Gung Memorial Hospital, Chiayi, Taiwan; [2]Department of General Surgery, Chang Gung Memorial Hospital, Taoyuan, Taiwan; [3]Department of Radiation Oncology, Chang Gung Memorial Hospital, Taoyuan, Taiwan. [*]Equal contributors.

Received June 13, 2023; Accepted August 27, 2023; Epub October 15, 2023; Published October 30, 2023

Abstract: This study aimed to investigate the dose parameters and incidence of radiotherapy (RT)-associated toxicity in patients with left breast cancer (LBC) treated with proton-RT, compared with photon-RT. We collected data from 111 patients with LBC who received adjuvant RT in our department between August 2021 and March 2023. Among these patients, 24 underwent proton-RT and 87 underwent photon-RT. In addition to the dosimetric analysis for organs at risk (OARs), we measured NT-proBNP levels before and after RT. Our data showed that proton-RT improved dose conformity and reduced doses to the heart and lungs and was associated with a lower rate of increased NT-proBNP than did photon-RT. Regarding skin toxicity, the Dmax for 1 c.c. and 10 c.c. and the average dose to the skin-OAR had predictive roles in the risk of developing radiation-induced dermatitis. Although pencil beam proton-RT with skin optimization had a dose similar to that of skin-OAR compared with photon-RT, proton-RT still had a higher rate of radiation dermatitis (29%) than did photon RT (11%). Using mice 16 days after irradiation, we demonstrated that proton-RT induced a greater increase in interleukin 6 and transforming growth factor-β1 levels than did photon-RT. Furthermore, topical steroid ointment reduced the inflammatory response and severity of dermatitis induced by RT. In conclusion, we suggest that proton-RT with skin optimization spares high doses to OARs with acceptable skin toxicity. Furthermore, prophylactic topical steroid treatment may decrease radiation dermatitis by alleviating proton-induced inflammatory responses in vivo.

Keywords: Breast cancer, proton therapy, photon radiotherapy, dermatitis

Introduction

Adjuvant radiotherapy (RT) is administered to patients with breast cancer at a significant risk of locoregional recurrence and has been demonstrated to have a survival benefit [1, 2]. However, RT-induced injuries including skin, lung, and heart toxicities have been noted [3-5]. A higher irradiated volume or absorbed dose is a risk factor for the development of RT-induced heart disease and pneumonitis. To improve target coverage and spare organs at risk (OARs) in breast cancer, photon-RT has evolved from conventional RT to intensity-modulated RT (IMRT) and volumetric RT (VMAT). According to the findings of our previous study, compared with conventional RT, IMRT leads to improved dose homogeneity with fewer radiation hotspots [6, 7].

In recent decades, proton-RT has become an established alternative to photon RT for treating specific types of cancer [8]. The application of proton-RT in the treatment of breast cancer has grown tremendously in the past few years because of technological advances and increasing recognition of the potential late sequelae of breast RT. Proton-RT has unique physical properties that reduce dose deposition outside the target volume. It can improve target coverage, particularly in the internal mammary chain, and limit heart and lung exposure [9, 10]. Beyond the dosimetric advantages, there has been great interest in the clinical outcomes of proton

Table 1. Characteristics of patients with left-sided breast cancer

	No. of patients		*p* value
	photon	proton	
Patients	87	24	
Age			
Median ± SD	54.8 ± 10.4	53 ± 9.2	0.311
BMI			0.398
<24	44	12	
≥24	43	12	
Risk factors			0.866
No	56		
Yes	31		
Stage			0.12
Tis-T2 N0	54	19	
≥T3 or N1	33	5	
Surgery type			0.34
Partial mastectomy	73	22	
Simple mastectomy	14	2	
RT dose			0.172
Hypofractionation	56	19	
Conventional	31	5	
Nodal irradiation			0.12
No	50	18	
Yes	37	6	
Hormone therapy			0.701
No	29	7	
Yes	58	17	
Dosimetry (mean ± SD)			
CTV-V95%	98 ± 0.28%	99 ± 0.3%	0.002*
CTV-V99%	94 ± 0.65%	96 ± 0.4%	<0.001*

*Statistical significance.

therapy. A better understanding of dose parameters and their relationship with RT-induced side effects will help improve the quality of life of patients after treatment. Therefore, this study analyzed the dose metrics of OARs and related acute toxicity in patients with left breast cancer (LBC) who underwent proton-RT, compared with IMRT/VMAT, at our institution.

Materials and methods

Patient characteristics and treatment techniques

This prospective study was approved by the institutional review board of Chang Gung Memorial Hospital (No. 202100807B0). Informed consent forms were signed by patients prior to their participation. In total, 111 patients with LBC who received adjuvant RT at our department between August 2021 and March 2023 were enrolled. The standard adjuvant RT dose was 50 Gy in 25 fractions (conventional regimen) or 42.56 Gy in 16 fractions (hypofractionation regimen). The clinical characteristics of the patients are shown in **Table 1**.

In this study, 24 patients underwent proton-RT and 87 patients underwent photon-RT (IMRT/VMAT). Among the enrolled patients, 65 received neoadjuvant or adjuvant chemotherapy sequentially with RT. Acute dermatitis was scored weekly using the RTOG skin toxicity scale, and 2 and 4 weeks after the end of radiotherapy. after completing RT. We examined the percentage of patients with ≥ grade 2 acute skin toxicity-classified as radiation dermatitis (RID)-and identified RID-related risk factors. In addition, we measured NT-proBNP, C-reactive protein, and troponin I levels before and after RT to evaluate radiation-induced acute heart inflammation.

Computed tomography simulation and treatment planning

For patients with LBC receiving adjuvant RT, the skin, heart, left anterior descending artery (LAD), and lungs were defined as the OARs. The clinical target volume (CTV) was expanded by 5 mm but was within 3 mm of the skin surface to create the PTV generated on the CT images. The criterion of the plan was to satisfy at least 95% of the prescription dose to cover 98% of the CTV, while minimizing the dose delivered to the OARs and contralateral breast. For the patients treated with hypofractionation regimen, the dose to OARs was corrected [11, 12]. For the enrolled patients who received proton therapy at our institute, it was delivered via intensity-modulated proton therapy (IMPT) with skin optimization using the skin OAR. The IMPT plans were generated using the Eclipse planning system (Varian Medical Systems, Palo Alto, CA, USA) with a pencil beam scanning (PBS) system. Two beam angles were used in the IMPT plan. The pre-

scribed dose was 50/42.56 Gy (relative biological effectiveness [RBE]). An RBE value of 1.1 was assumed for protons [13]. At our hospital, proton therapy was delivered using a cyclotron (Sumitomo Heavy Industries, Ltd.) that generated a continuous and high-intensity proton beam.

Treatment planning and in silico analysis

We collected the CT simulation data from the first 16 patients with LBC undergoing postoperative proton therapy for in silico analysis. The breast target and OAR structures were contoured on CT images. In addition, one pseudo-skin structure was defined as a 3 mm deep layer (skin-OAR). For each patient, four classes of plans were generated: a VMAT plan and three proton plans (passive scattering proton therapy [PSPT], IMPT1, and IMPT2). For all patients, the prescribed dose was 50 Gy (RBE) in 2 Gy daily fractions. Proton therapy plans were generated using the Eclipse planning system as described above. Each patient had three different proton therapy plans with the same objectives and constraints, except for the skin OAR. For the proton therapy plans, the dose to the target was delivered using the PSPT technique in the first PSPT plan and the IMPT technique in the IMPT1 plan. In the fourth plan (IMPT2), the pseudo-skin structure (skin-OAR) was added to the optimization as an objective at a maximum prescribed dose using the IMPT technique. For each patient, dose-volume histograms (DVHs) from the planning data were extracted for analysis.

Mice, RT and topical therapy

The protocols for animal experimentation were approved by the Laboratory Animal Center of our hospital (No. 2023030303). We used 8-week-old C57BL/6 female mice purchased from the National Science Council to establish a RT-induced dermatitis model. The model mimics the dosimetry features of adjuvant RT observed in the skin of patients without gross tumor; therefore, this model should be advantageous for studies of the immune response in RT-induced toxicity. The mice received local RT by either photon or proton irradiation at the same RBE dose [7, 14]. Photon irradiation was performed using Varian 21EX and proton irradiation was performed using PBS. For photon irradiation, the skin of the anesthetized mice was covered with a 0.3 cm bolus. To examine the response of the skin to PT, compared with photon irradiation, in vivo, local irradiation at 12 Gy (RBE) was administered to the lower back. Proton irradiation was delivered by the cyclotron used at our hospital (Sumitomo Heavy Industries, Ltd.). We observed skin reactions at the indicated time points. To investigate the effects of topical steroid treatment on RT-induced dermatitis, the irradiated mice were administered a topical steroid ointment immediately after RT irradiation and every 2 days until the end of the experiments. We obtained skin biopsies for real-time reverse transcription-polymerase chain reaction (RT-PCR), immunofluorescence (IF), and immunochemical (IHC) staining at the indicated times. Real-time RT-PCR for IL-6 and TGF-β1 was performed using RNA extracted from the tissue specimen and the SYBR Green qPCR Master Mix. Formalin-fixed, paraffin-embedded tissues were cut into 5-mm sections and mounted on slides for IHC staining. Frozen tissue specimens were cut into 5-8 μm cryostat sections. The sections were incubated overnight at 4°C with antibodies against the target protein, washed, and incubated for 1 h with fluorescein or Texas Red-conjugated secondary antibodies. The slides were counterstained with DAPI to visualize the nuclei. The positive staining signals were assessed by microscope from ten random fields and semi-quantitated by MetaMorph software.

Statistical analysis

Student's t-tests were used to analyze the associations between RT-induced toxicity, dosimetric parameters, and clinical characteristics and to compare the dose distribution between the plans. Dose reduction to the OAR was compared between the VMAT and proton therapy plans. *P*-values for two-tailed tests with a 95% confidence interval was used. Linear regression analyses were performed using SPSS version 17.0. In addition, for the in vivo experiments, six animals were used per group and at least two independent experiments were performed. A probability level of $P<0.05$ was taken to indicate statistical significance. Samples were analyzed using Student's t-test. Data are presented as the mean ± standard error of the mean (SD).

Table 2A. Dosimetric differences between photon-RT and proton-RT for OAR

	Photon-RT	Proton-RT	*p* value
Heart			
Dmean (cGy)	305.31 ± 12.56	15.65 ± 2.61	<0.001*
V2 Gy (%)	41.22 ± 2.57%	1.77 ± 0.26%	<0.001*
V5 Gy (%)	12.91 ± 0.83%	0.79 ± 0.15%	<0.001*
V10 Gy (%)	5.5 ± 0.42%	0.3 ± 0.09%	<0.001*
V20 Gy (%)	1.93 ± 0.25%	0.09 ± 0.04%	<0.001*
LAD			
Dmean (cGy)	1699 ± 101	88 ± 20	<0.001*
V20 Gy (%)	34.8 ± 3.5%	0.06 ± 0.06%	<0.001*
V30 Gy (%)	10.05 ± 2.43%	0%	0.032*
Left Lung			
Dmean (cGy)	966 ± 26	212 ± 32	<0.001*
V5 Gy (%)	39.9 ± 0.93%	13.1 ± 2%	<0.001*
V20 Gy (%)	17.87 ± 0.7%	2.58 ± 0.9%	<0.001*
Whole Lung			
Dmean (cGy)	505 ± 14	125 ± 33	<0.001*
V5 Gy (%)	20.33 ± 1%	6.25 ± 1%	<0.001*
V20 Gy (%)	8.2 ± 0.4%	1.2 ± 0.4%	<0.001*

*Statistical significance.

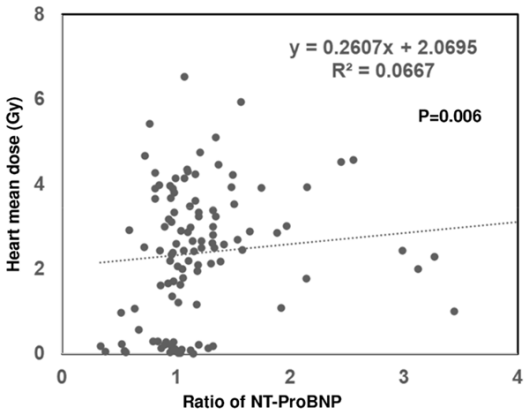

Figure 1. Relationship between heart mean dose and the ratio of NT-ProBNP for left-sided breast cancer patients. The x axis represents the relative fold change in the value of NT-ProBNP after RT.

Results

The clinical characteristics of the enrolled 111 patients are listed in **Table 1**.

Dosimetric parameters of OARs and related changes in heart inflammation markers

Table 2A summarizes the dose parameters of the OARs (heart, LAD, and lungs). Treatment with proton-RT was associated with lower lung V5 and V20 and average dose for the ipsilateral and bilateral lungs. The lung mean dose values for the photon-RT and proton-RT groups were 966 ± 26 cGy and 212 ± 32 cGy, respectively (P<0.001). Regarding the heart irradiated dose, patients treated with proton-RT had significantly lower cardiac exposure, including the mean heart dose and V2-V20, according to the DVH data extracted from the planning system. Reportedly, the heart dose volumes are correlated with late cardiac events. Furthermore, cardiac biomarkers such as troponin and NT-proBNP levels reportedly increase after RT and correlate with clinical outcomes in patients with heart failure [15-17]. In the present study, we measured pro-BNP and troponin I levels before and at the end of RT. Our data revealed that increased levels of NT-proBNP were related to the mean heart dose (**Figure 1**), V2, and V5. In addition, the correlation between a significant increase in pro-BNP (≥10% increase) levels and the examined risk factors was calculated. There was a lower significant increase in the NT-proBNP levels in the proton group than in the photon group, which was associated with a lower mean dose to the heart and LAD (**Table 2B**).

Skin dose related to proton therapy planning

According to a reported series, an almost doubled rate of acute skin toxicity (i.e., RID) was noted after PT, compared with photon irradiation, although PBS techniques were used [18-20]. To objectively measure the skin dose delivered by photon VMAT plans and both IMPT and PSPT plans, the enrolled proton patients had dedicated research skin contours created within their respective RT planning systems. A pseudo-skin contour (skin-OAR) was measured as a rind extending 3 mm inward from the external contour encompassed within the 50% isodose line representative of the radiation field edge. As shown in **Table 3A** and **Figure 2**, the Dmax for 1 c.c. and 10 c.c. and the mean dose to the skin-OAR were significantly higher in PSPT than in VMAT. We further analyzed dosimetry via IMPT by minimizing the volume of

Table 2B. Factors correlated with the RT-induced significant increase of Pro-BNP

	Increase of Pro-BNP		*p* value
	<10%	≥10%	
Patients	57	54	
BMI			0.502
<24	29	24	
≥24	29	30	
Risk factors			0.857
No	36	35	
Yes	21	19	
RT technique			0.002*
Photon	38	49	
Proton	19	5	
Nodal irradiation			0.677
No	36	32	
Yes	21	22	
Hormone therapy			0.543
No	20	16	
Yes	39	38	
Chemotherapy			0.089
No	26	20	
Yes	31	34	
Dosimetry			
Heart			
Mean dose (cGy)	203.4 ± 22.3	284.2 ± 18.6	0.007*
V2 (%)	25.75 ± 3.37%	40.00 ± 3.58%	0.005*
V5 (%)	8.56 ± 1.09%	12.10 ± 1.14%	0.027*
V10 (%)	3.72 ± 0.56%	5.03 ± 0.53%	0.095
V20 (%)	1.38 ± 0.28%	1.69 ± 0.30%	0.439
LAD			
Mean dose (cGy)	1115.1 ± 133.3	1600.7 ± 147.5	0.016*
V20 (%)	20.57 ± 3.89%	34.51 ± 4.71%	0.024*
V30 (%)	5.38 ± 2.13%	10.51 ± 3.27%	0.188

*Statistical significance.

the prescribed dose delivered to the skin-OAR. As shown in **Table 3A**, IMPT with skin-OAR optimization had a better target coverage and a lower irradiated volume associated with similar doses to the skin than did VMAT. We have added the criteria for skin-OAR for the enrolled patients who received proton therapy.

Factors related to skin toxicity induced by RT

Figure S1 shows representative images of grade 1 and 2 acute skin toxicities. RID (≥ grade 2 skin toxicity) was noted in 17 of the 111 patients (15.3%). None of the patients who developed RID had grade 3 RID. Our results (**Table 3B**) indicate that simple mastectomy, elective nodal irradiation, and proton therapy increased the risk of grade 2 RID. The incidence of grade 2 RID was 1.5% (1/68) in the patients who did not receive regional nodal irradiation and 37% (16/43) in those who did (P<0.001). Furthermore, there was a higher rate of RID in patients receiving proton therapy (29%; 7/24) than in those receiving photon RT (11%; 10/87) (P=0.033). **Table 3B** shows that the Dmax for 1 c.c. and 10 c.c. and the mean dose to the skin-OAR have a predictive role in the risk of developing RID. On the basis of the dosimetric analysis, we found no significant difference in the mean dose (36.57 ± 0.47 Gy *vs* 37.5 ± 0.38 Gy; *P*=0.234), Dmax 1 c.c. (42.18 ± 0.51 Gy *vs* 43.17 ± 0.26 Gy; *P*=0.083), and Dmax 10 c.c. (40.86 ± 0.47 Gy *vs* 40.93 ± 0.25 Gy; *P*=0.898) to the skin-OAR between the photon and proton therapy groups, respectively.

Biologic changes related to RID

Most in vivo studies on RID are photon therapy-related. In the present study, we found that the incidence of RID induced by IMPT with skin optimization was higher than that induced by photon-RT. Accordingly, we examined the related biologic changes induced by proton compared with photon therapy. RID is mediated by the induction of cell death and inflammation [21, 22]. This mechanism is either directly or indirectly associated with DNA damage. Acute RID in vivo has been reported obviously on D7-D14. Accordingly, we examined the skin response to proton therapy in vivo for 16 days after irradiation. As shown in Figure S2, proton-RT induced increased cell death 2 days after irradiation, which was associated with significantly higher levels of interleukin (IL)-6 and transforming growth factor (TGF)-β1-important mediators of radiation-induced inflammation-in the RT groups than in the sham-irradiated group. The increase in inflammatory cytokine

Table 3A. Dosimetric differences between 4 RT plans for skin-OAR

	Plan 1 (VMAT)	Plan 2 (PSPT)	*P value* (plan 1 *versus* 2)	Plan 3 (IMPT without skin-OAR)	*P value* (plan 1 *versus* 3)	Plan 4 (IMPT with skin-OAR)	*P value* (plan 1 *versus* 4)
Skin OAR							
Dmean (Gy)	34.18 ± 0.39	43.61 ± 0.47	<0.001*	37.32 ± 0.33	<0.001*	35.23 ± 0.45	0.082
V100 (%)	0.001 ± 0.001	58.66 ± 2.47	<0.001*	0.47 ± 0.35	0.183	0.064 ± 0.062	0.325
Dmax (1 c.c.)	41.56 ± 0.39	47.54 ± 0.36	<0.001*	43.53 ± 0.35	0.001*	41.2 ± 0.41	0.532
Dmax (10 c.c.)	39.46 ± 0.38	47.01 ± 0.35	<0.001*	42.39 ± 0.36	<0.001*	40.01 ± 0.41	0.336
CTV							
V95%	99.66 ± 0.09	99.84 ± 0.07	0.128	99.78 ± 0.09	0.389	99.49 ± 0.10	0.242
V99%	92.2 ± 0.38	98.50 ± 0.41	<0.001*	99.18 ± 0.27	<0.001*	95.73 ± 0.40	<0.001*
V50%/CTV	5.17 ± 0.30	2.95 ± 0.12	<0.001*	2.94 ± 0.12	<0.001*	2.84 ± 0.12	<0.001*

*Statistical significance.

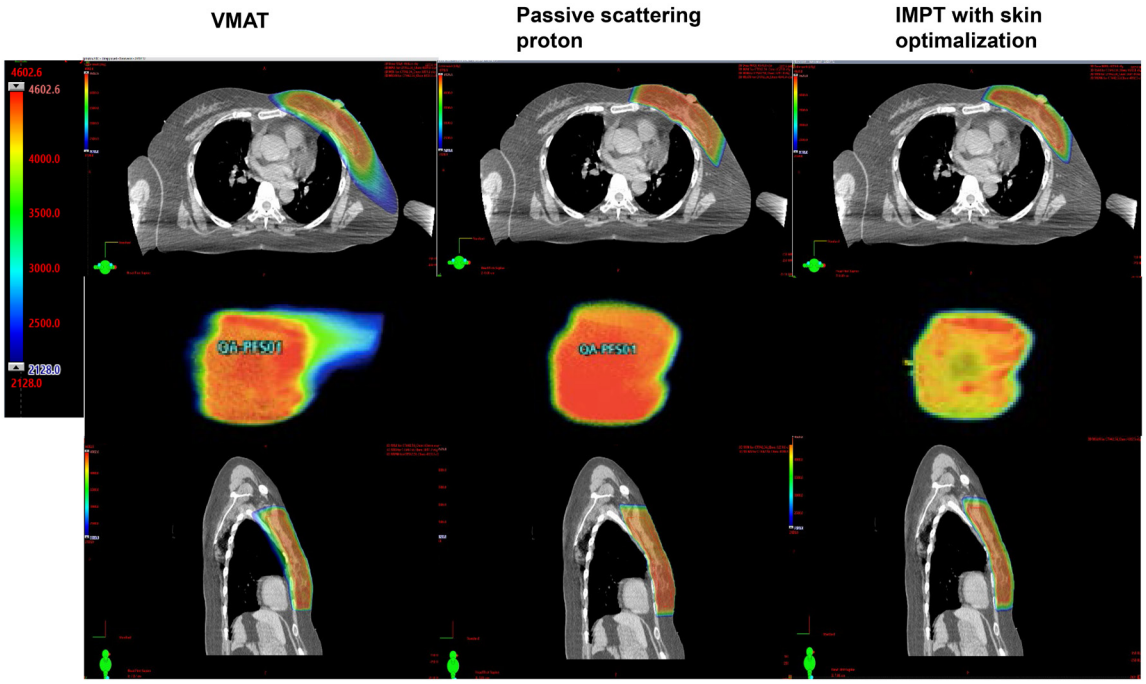

Figure 2. The isodose distributions in silico analysis are presented for a representative patient.

levels induced by photon-RT was similar to that induced by proton-RT 48 h after irradiation. The data obtained from mice 16 days after RT (**Figures 3** and S2) revealed that protons induced a greater increase in inflammatory mediators than did photons, which was associated with slower hair regrowth in the irradiated area. Moreover, **Figure 3** shows that the application of topical steroid agents reduced the severity of RID and alleviated the RT-induced inflammatory response.

Discussion

Radiation dosimetry research has demonstrated that proton therapy provides better target conformity and simultaneous reduction in the surrounding normal tissues receiving a higher irradiation dose than photon-RT [23, 24]. Further investigation of the dose parameters and incidence of radiation-associated toxicity will help select patients who would benefit most from proton therapy.

Table 3B. Factors correlated with the RT-induced skin toxicity

	Skin toxicity		*p* value
	< Grade 2	≥ Grade 2	
Patients	94	17	
BMI			0.645
<24	44	9	
≥24	50	8	
Surgery type			0.007*
Partial mastectomy	84	11	
Simple mastectomy	10	6	
H/T			0.787
No	30	6	
Yes	64	11	
RT technique			0.033*
Photon	77	10	
proton	17	7	
Nodal irradiation			<0.001*
No	67	1	
Yes	27	16	
Skin-OAR			
Dmean (Gy)	36.62 ± 0.31	41.08 ± 0.66	<0.001*
Dmax 1 c.c. (Gy)	42.17 ± 0.14	47.33 ± 0.66	<0.001*
Dmax 10 c.c.	40.18 ± 0.13	45.00 ± 0.62	<0.001*
V100 (%)	0.009 ± 0.005	0.000 ± 0.000	0.499

*Statistical significance.

The International Commission on Radiological Protection reported that a dose of 0.5 Gy might lead to ~1% of exposed individuals developing cardiovascular disease >10 years after exposure [25]. The mean heart dose is the principal planning parameter used in breast cancer RT [3, 11, 26]. As the incidence of coronary heart disease is proportional to the mean dose, the dose to the heart should be reduced as much as possible. In addition, the dose to the coronary artery subsegments has also been correlated with major coronary events [27], and the LAD is an important structure in RT-related heart abnormalities. When LAD Dmean above 2.8 Gy, the risk for any cardiac event was higher [28]. In our previous study, patients treated with IMRT had a significantly lower average heart dose and V5-V20 than did those treated with conventional RT for LBC [6]. A regimen using IMRT and the deep inspiration-breath-hold technique further decreased the mean dose to the heart and LAD. However, the potential risk associated with IMRT and VMAT is that these techniques expose the heart to a substantial "low dose bath" from multiple beam angles. Furthermore, the deep inspiration-breath-hold technique had no significant impact on dose reduction in the lungs and did not benefit all patients in decreasing the mean heart dose [12]. In the present study, we demonstrated that proton therapy, compared with photon-RT, significantly reduced the dose to the heart, LAD and lungs in patients with LBC. The use of early markers of radiation-associated cardiac damage may enable improved prediction and mitigation of late cardiac toxicity from breast RT [15]. NT-proBNP is significantly associated with cardiotoxic reactions. The active and inactive (pro-BNP and NT-proBNP) forms of BNP are classically used as biomarkers for diagnosing and monitoring acute and chronic heart failure. An early increase in NT-pro-BNP levels has been reported to be correlated with cardiotoxic reactions. Furthermore, BNP levels increase significantly after serial dosing during RT [16, 17]. In the present study, we measured pro-BNP levels before and at the end of RT in 111 patients with LBC and considered an increase of >10% to be significant. Our data revealed that a significant increase from baseline occurred in 49% of the patients after RT. A significant increase in NT-proBNP levels was associated with a higher irradiation dose to the heart and LAD. However, no significant changes in troponin I levels were observed after RT. Since the anatomical and functional alterations induced by RT usually occur extremely late, a longer follow-up is needed to demonstrate a correlation between the alterations in biomarkers and the development of cardiovascular disease in the future.

RID is a commonly reported toxicity associated with radiation exposure to the breast and chest wall. Despite documented improvements in cardiac and pulmonary dosimetry, some studies have reported that the rates of RID were significantly elevated in the proton therapy cohort compared with those in the photon-RT cohort [18-20, 29]. There are concerns regarding radiation-induced skin toxicities, given the

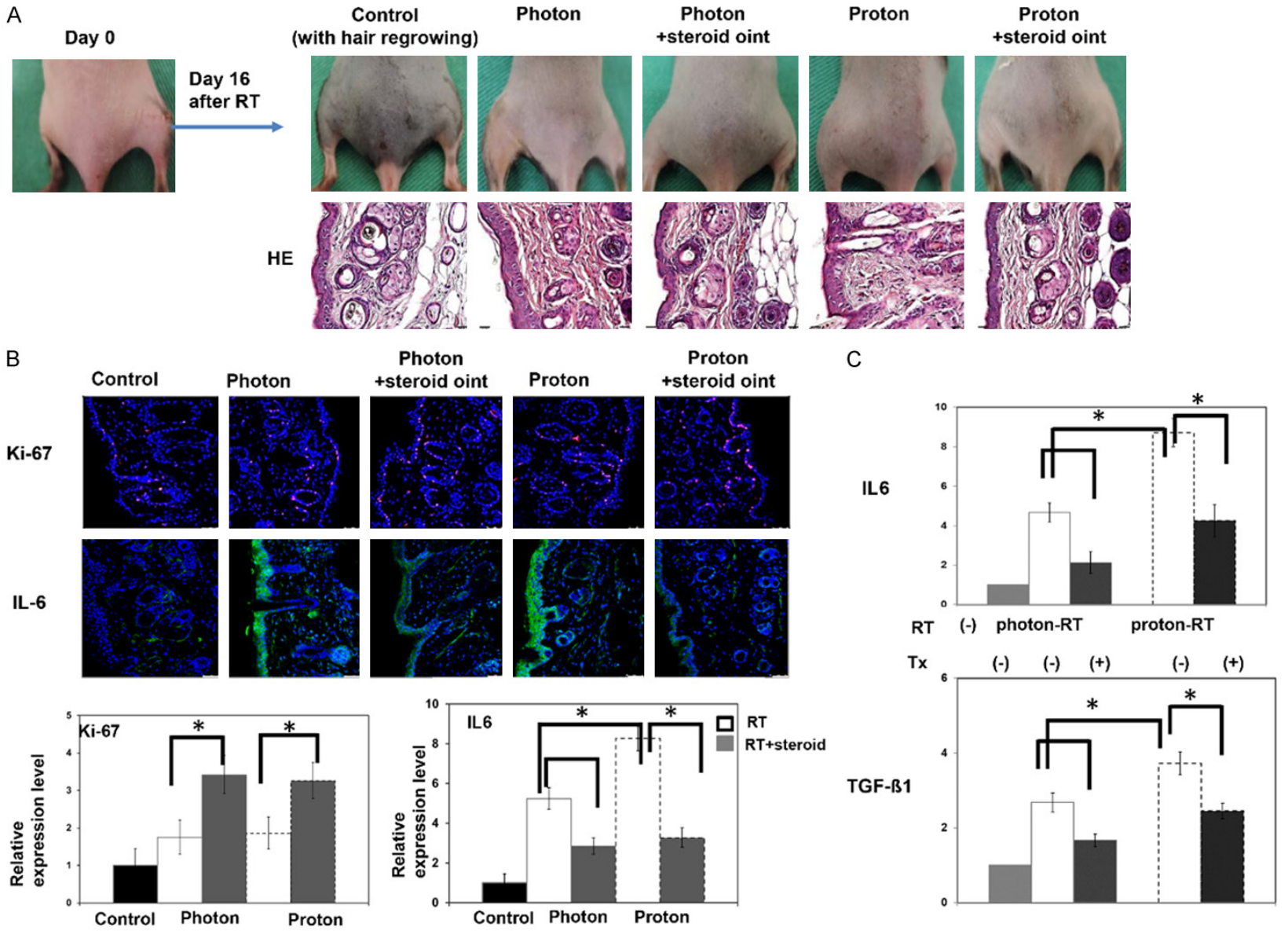

Figure 3. The effect of topical steroid ointment on radiation dermatitis following RT. A. Representative pictures of irradiated skin and HE staining 16 days after RT (Scale bar =20 um). B. Immunofluorescence for ki-67 and IL-6 are shown by representative slides and quantitative data 16 days after RT (DAPI, blue; IL-6, green;

ki-67, red). Scale bar: 50 um. The y axis represents the relative fold changes in the target protein ex-pressions. C. The levels of IL-6 and TGF-ß1 were examined via real-time RT-PCR16 days after RT. The y axis represents the relative fold change in the value of target proteins. Data are presented as means ± standard errors of the mean. *, P<0.05.

higher skin dose related to a proton beam than to a photon beam. However, the reported toxicities are mainly due to passive scattering. Nowadays, with IMPT delivered using PBS, a decreased dose to the skin surface can be expected owing to its higher modulation capability. Drawing conclusions regarding toxicity expectations from treatments delivered to different patients using various techniques is difficult. Accordingly, we defined a pseudo-skin structure as a 3 mm deep layer (skin-OAR) to analyze whether the dosimetric factors associated with IMPT caused differing effects from those of conventionally delivered photon beams. Using in silico analysis, the proton beam plans achieved greater target coverage than did the VMAT plan in all patients. Regarding skin sparing, the data revealed that compared with the VMAT plan, the proton plan with the PSPT technique resulted in the highest dose delivered to the pseudo-skin structures. Furthermore, IMPT plans with skin optimization allowed similar dosimetry to be obtained on the pseudo-skin structure as in the VMAT plan with increased target coverage. In the present study, although the incidence of RID was higher in patients treated with protons, the incidence of RID induced by protons was lower than that reported in other studies. According to our analysis, IMPT with skin sparing is a promising strategy to decrease the incidence of RID. DeCesaris et al. [20] reported a higher incidence of grade 2 RD in patients undergoing proton radiation for each corresponding photon Dmax on the basis of a dose-response curve after conversion. Therefore, we used mouse models to examine the biological effects induced by protons on the skin compared with those induced by photons. IL-6 and TGF-β1 have been reported as important predictive biological markers for RT-induced inflammation and fibrosis [30, 31]. Therefore, we examined IL-6/p-STAT3 and TGF-β1 activities at the indicated time points. The in vivo data showed that proton therapy induced higher levels of IL-6 and TGF-β1 expression on day 16 after irradiation than did photon therapy. Furthermore, compared with proton treatment alone, a combination of topical steroids attenuated the expression of IL-6 and TGF-β1. On the basis of the in vivo experiment results, proton-RT may induce more sustained inflammation than photon-RT does, and prophylactic topical steroid treatment inhibits RT-induced inflammation, leading to decreased radiation skin toxicity.

This study had a few limitations. It was a single-institute cohort study but lacked data on long-term follow-up for skin and cardiopulmonary toxicity. Therefore, a prospective trial with a longer follow-up period and more patients is needed. Moreover, the effects of proton therapy on the irradiated skin and the underlying mechanisms require further investigation.

Conclusion

In general, the choice of adjuvant RT and the method used are mainly based on individual characteristics and target regions. Our data suggest that proton therapy with skin optimization offers better dose conformity than does the VMAT technique and spares high-dose levels to OARs with acceptable skin toxicity in patients with LBC. Furthermore, prophylactic topical steroid treatment may decrease RID by alleviating proton-induced inflammatory responses in vivo.

Acknowledgements

The work was supported by Chang Gung Memorial Hospital. Grant CMRPG6J0183 (to C.C. Hsieh), and CORPG6L0032 (to M.F. Chen).

Informed consent forms were signed by patients prior to their participation.

Disclosure of conflict of interest

None.

Address correspondence to: Miao-Fen Chen, Department of Radiation Oncology, Chang Gung Memorial Hospital, Taoyuan, Taiwan. E-mail: miaofen@adm.cgmh.org.tw

References

[1] Clarke M, Collins R, Darby S, Davies C, Elphinstone P, Evans V, Godwin J, Gray R, Hicks C, James S, MacKinnon E, McGale P, McHugh T,

Peto R, Taylor C and Wang Y; Early Breast Cancer Trialists' Collaborative Group (EBCTCG). Effects of radiotherapy and of differences in the extent of surgery for early breast cancer on local recurrence and 15-year survival: an overview of the randomised trials. Lancet 2005; 366: 2087-106.

[2] EBCTCG (Early Breast Cancer Trialists' Collaborative Group); McGale P, Taylor C, Correa C, Cutter D, Duane F, Ewertz M, Gray R, Mannu G, Peto R, Whelan T, Wang Y, Wang Z and Darby S. Effect of radiotherapy after mastectomy and axillary surgery on 10-year recurrence and 20-year breast cancer mortality: meta-analysis of individual patient data for 8135 women in 22 randomised trials. Lancet 2014; 383: 2127-35.

[3] Darby SC, Ewertz M, McGale P, Bennet AM, Blom-Goldman U, Bronnum D, Correa C, Cutter D, Gagliardi G, Gigante B, Jensen MB, Nisbet A, Peto R, Rahimi K, Taylor C and Hall P. Risk of ischemic heart disease in women after radiotherapy for breast cancer. N Engl J Med 2013; 368: 987-98.

[4] Pignol JP, Olivotto I, Rakovitch E, Gardner S, Sixel K, Beckham W, Vu TT, Truong P, Ackerman I and Paszat L. A multicenter randomized trial of breast intensity-modulated radiation therapy to reduce acute radiation dermatitis. J Clin Oncol 2008; 26: 2085-92.

[5] Vogelius IR and Bentzen SM. A literature-based meta-analysis of clinical risk factors for development of radiation induced pneumonitis. Acta Oncol 2012; 51: 975-83.

[6] Chen CH, Hsieh CC, Chang CS and Chen MF. A retrospective analysis of dose distribution and toxicity in patients with left breast cancer treated with adjuvant intensity-modulated radiotherapy: comparison with three-dimensional conformal radiotherapy. Cancer Manag Res 2020; 12: 9173-82.

[7] Chen MF, Chen WC, Lai CH, Hung CH, Liu KC and Cheng YH. Predictive factors of radiation-induced skin toxicity in breast cancer patients. BMC Cancer 2010; 10: 508.

[8] Doyen J, Falk AT, Floquet V, Herault J and Hannoun-Levi JM. Proton beams in cancer treatments: clinical outcomes and dosimetric comparisons with photon therapy. Cancer Treat Rev 2016; 43: 104-12.

[9] Braunstein LZ and Cahlon O. Potential morbidity reduction with proton radiation therapy for breast cancer. Semin Radiat Oncol 2018; 28: 138-49.

[10] Kammerer E, Guevelou JL, Chaikh A, Danhier S, Geffrelot J, Levy C, Saloux E, Habrand JL and Thariat J. Proton therapy for locally advanced breast cancer: a systematic review of the literature. Cancer Treat Rev 2018; 63: 19-27.

[11] Gagliardi G, Constine LS, Moiseenko V, Correa C, Pierce LJ, Allen AM and Marks LB. Radiation dose-volume effects in the heart. Int J Radiat Oncol Biol Phys 2010; 76 Suppl: S77-85.

[12] Chang CS, Chen CH, Liu KC, Ho CS and Chen MF. Selection of patients with left breast cancer for IMRT with deep inspiration breath-hold technique. J Radiat Res 2020; 61: 431-9.

[13] Paganetti H. Relative biological effectiveness (RBE) values for proton beam therapy. Variations as a function of biological endpoint, dose, and linear energy transfer. Phys Med Biol 2014; 59: R419-72.

[14] Chen MF, Chen PT, Hsieh CC and Wang CC. Effect of proton therapy on tumor cell killing and immune microenvironment for hepatocellular carcinoma. Cells 2023; 12: 332.

[15] Semeraro GC, Cipolla CM and Cardinale DM. Role of cardiac biomarkers in cancer patients. Cancers (Basel) 2021; 13: 5426.

[16] Forte M, Madonna M, Schiavon S, Valenti V, Versaci F, Zoccai GB, Frati G and Sciarretta S. Cardiovascular pleiotropic effects of natriuretic peptides. Int J Mol Sci 2019; 20: 3874.

[17] Skytta T, Tuohinen S, Luukkaala T, Virtanen V, Raatikainen P and Kellokumpu-Lehtinen PL. Adjuvant radiotherapy-induced cardiac changes among patients with early breast cancer: a three-year follow-up study. Acta Oncol 2019; 58: 1250-8.

[18] Cuaron JJ, Chon B, Tsai H, Goenka A, DeBlois D, Ho A, Powell S, Hug E and Cahlon O. Early toxicity in patients treated with postoperative proton therapy for locally advanced breast cancer. Int J Radiat Oncol Biol Phys 2015; 92: 284-91.

[19] Liang X, Bradley JA, Zheng D, Rutenberg M, Yeung D, Mendenhall N and Li Z. Prognostic factors of radiation dermatitis following passive-scattering proton therapy for breast cancer. Radiat Oncol 2018; 13: 72.

[20] DeCesaris CM, Rice SR, Bentzen SM, Jatczak J, Mishra MV and Nichols EM. Quantification of acute skin toxicities in patients with breast cancer undergoing adjuvant proton versus photon radiation therapy: a single institutional experience. Int J Radiat Oncol Biol Phys 2019; 104: 1084-90.

[21] Sheng X, Zhou Y, Wang H, Shen Y, Liao Q, Rao Z, Deng F, Xie L, Yao C, Mao H, Liu Z, Peng M, Long Y, Zeng Y, Xue L, Gao N, Kong Y and Zhou X. Establishment and characterization of a radiation-induced dermatitis rat model. J Cell Mol Med 2019; 23: 3178-89.

[22] Liao W, Hei TK and Cheng SK. Radiation-induced dermatitis is mediated by IL17-expressing gammadelta T cells. Radiat Res 2017; 187: 454-64.

[23] Fontanilla HP, Woodward WA, Lindberg ME, Kanke JE, Arora G, Durbin RR, Yu TK, Zhang L, Sharp HJ, Strom EA, Salehpour M, White J, Buchholz TA and Dong L. Current clinical coverage of Radiation Therapy Oncology Group-defined target volumes for postmastectomy radiation therapy. Pract Radiat Oncol 2012; 2: 201-9.

[24] Lin LL, Vennarini S, Dimofte A, Ravanelli D, Shillington K, Batra S, Tochner Z, Both S and Freedman G. Proton beam versus photon beam dose to the heart and left anterior descending artery for left-sided breast cancer. Acta Oncol 2015; 54: 1032-9.

[25] Authors on behalf of ICRP; Stewart FA, Akleyev AV, Hauer-Jensen M, Hendry JH, Kleiman NJ, Macvittie TJ, Aleman BM, Edgar AB, Mabuchi K, Muirhead CR, Shore RE and Wallace WH. ICRP statement on tissue reactions and early and late effects of radiation in normal tissues and organs--threshold doses for tissue reactions in a radiation protection context. Ann ICRP 2012; 41: 1-322.

[26] Taylor C, Correa C, Duane FK, Aznar MC, Anderson SJ, Bergh J, Dodwell D, Ewertz M, Gray R, Jagsi R, Pierce L, Pritchard KI, Swain S, Wang Z, Wang Y, Whelan T, Peto R and McGale P; Early Breast Cancer Trialists' Collaborative Group. Estimating the risks of breast cancer radiotherapy: evidence from modern radiation doses to the lungs and heart and from previous randomized trials. J Clin Oncol 2017; 35: 1641-9.

[27] Banfill K, Giuliani M, Aznar M, Franks K, McWilliam A, Schmitt M, Sun F, Vozenin MC and Faivre Finn C; IASLC Advanced Radiation Technology committee. Cardiac toxicity of thoracic radiotherapy: existing evidence and future directions. J Thorac Oncol 2021; 16: 216-27.

[28] Zureick AH, Grzywacz VP, Almahariq MF, Silverman BR, Vayntraub A, Chen PY, Gustafson GS, Jawad MS and Dilworth JT. Dose to the left anterior descending artery correlates with cardiac events after irradiation for breast cancer. Int J Radiat Oncol Biol Phys 2022; 114: 130-9.

[29] Verma V, Shah C and Mehta MP. Clinical outcomes and toxicity of proton radiotherapy for breast cancer. Clin Breast Cancer 2016; 16: 145-54.

[30] Herskind C, Bamberg M and Rodemann HP. The role of cytokines in the development of normal-tissue reactions after radiotherapy. Strahlenther Onkol 1998; 174 Suppl 3: 12-5.

[31] Muller K and Meineke V. Radiation-induced alterations in cytokine production by skin cells. Exp Hematol 2007; 35 Suppl 1: 96-104.

Figure S1. Representative pictures of selected patients with grade 1 and 2 acute skin toxicity.

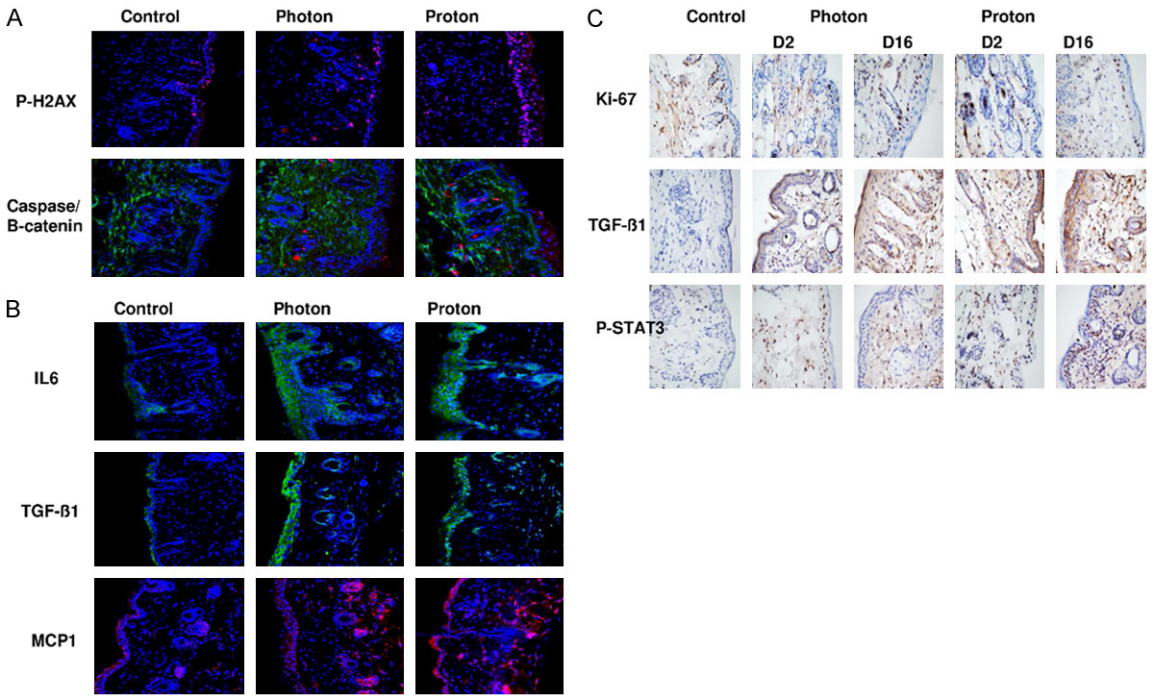

Figure S2. Response of murine skin to RT in vivo. A. Immunofluorescence for RT-induced DNA damage and cell death are shown by representative slides 48 h after RT (DAPI, blue; pH2AX and cleavage caspase 3, red; β-catenin, green). B. Immunofluorescence for IL-6, TGF-β1 and MCP1 are shown by representative slides 48 h after RT (DAPI, blue; IL-6, TGF-β1, green; MCP1, red). C. Immunochemical staining for ki-67, TGF-β1, and p-stat3 are shown by representative slides 48 h and 16 days after RT.